

Assessing Chemical Heterogeneity at the Nanoscale in Mixed-Ligand Metal-Organic Frameworks with the PTIR Technique

Aaron M. Katzenmeyer,¹ Jerome Canivet,² Glenn Holland,¹ David Farrusseng² and Andrea Centrone^{1*}

[*] Dr. A. M. Katzenmeyer, Mr. G. Holland, and Dr. A. Centrone
Center for Nanoscale Science and Technology National Institute of Standards and Technology
100 Bureau Drive, Gaithersburg, Maryland 20899, United States
E-mail: andrea.centrone@nist.gov

Dr. J. Canivet and Dr. D. Farrusseng
Institut de Recherches sur la Catalyse et l'Environnement de Lyon (IRCELYON) - Université Lyon 1, CNRS
2, Av. Albert Einstein F-69626 Villeurbanne
E-mail: david.farrusseng@ircelyon.univ-lyon1.fr

Supporting information for this article is available on the WWW under <http://www.angewandte.org> or from the author.

Abstract: *Recently, the use of mixtures of organic building block linkers gave chemists an additional degree of freedom for engineering Metal Organic Framework (MOF) properties; but the chemical complexity of such MixMOF structures is poorly characterized by conventional techniques, hindering verification of rational design. In this Communication the Photo Thermal Induced Resonance technique is applied to individual MixMOF micro-crystals to elucidate chemical composition with nanoscale resolution. Results show that MixMOFs isorecticular to In-MIL-68, obtained either directly from solution or by post-synthetic linker exchange, are homogeneous down to ≈ 100 nm. Additionally, we report a novel in situ process that enables engineering of anisotropic domains in MOF crystals with sub-micron linker concentration gradients.*

Metal-organic frameworks (MOFs), also known as porous coordination polymers, are crystalline, micro to mesoporous functional materials consisting of inorganic clusters interconnected by organic linkers. The possibility of tailoring the chemical functionality and pore size while maintaining the framework structure, a concept termed isorectularity,^[1] makes these materials promising for adsorption based processes,^[2] heat pumps,^[3] catalysis,^[4] and particularly photo-catalysis,^[5] gas storage,^[6] drug delivery,^[7] sensing^[8] and imaging.^[9] To target those applications isorecticular MOFs composed of mixtures of linkers, referred to as multivariate MOFs or MixMOFs, including core shell structures,^[10] is one of the latest

achievements in the field.^[4a, 6, 11] However, along with the benefits of multivariate MOF complexity comes the challenge of spatially resolving the distribution of the constituent building blocks within MOF crystallites. For example, homogeneity in the distribution of active or adsorption sites within a crystal is a prerequisite for the design of advanced catalytic materials^[12] or sensing. However, determining the chemical composition at the nanoscale in such materials remains elusive due to the limited spatial resolution of conventional techniques. This lack of spatially resolved information hinders fundamental understanding of these materials and consequently the ability to engineer them for greatest efficacy. In this work, the local chemical composition of individual MixMOF micro-crystals is determined for the first time with nanoscale resolution using the Photo Thermal Induced Resonance (PTIR) technique,^[13] a novel method that combines the lateral resolution of atomic force microscopy (AFM) with the chemical specificity of infrared (IR) spectroscopy (Figure 1). PTIR experiments show that MixMOFs isorecticular to In-MIL-68,^[14] made either directly from solution or by post-synthetic linker exchange are homogeneous down to a length scale of ≈ 100 nm. Additionally, an *in situ* process for engineering anisotropic domains in MOF crystals is reported, leading to a linker concentration gradient occurring within ≈ 600 nm.

MixMOF characterization has been attempted with a variety of techniques. High resolution XRD was used to demonstrate the homogeneity of “mixed” Al-MIL-53^[11a] and MOF-5^[4a] crystals in which the terephthalate (bdc) linker is partially substituted by 2-amino-terephthalate (abdc). However, powder XRD cannot assess linker gradients within a crystal or distinguish a physical mixture of crystals from chemically distinct domains within a crystal. Visible images and IR micro-spectroscopy were used to prove the formation of a MOF (crystals >200 μm) where two linkers form phase separated domains.^[15] However, the resolution of these techniques, is insufficient for many technologically relevant MOFs which grow preferentially as nano or micro-crystals or in applications where large crystals may be undesirable. Energy dispersive X-ray spectroscopy was used to assess MOF elemental composition with submicron resolution,^[16] but this technique cannot identify functional groups nor confirm the incorporation of the linker(s) in the MOF structure. Furthermore, electron beams are known to damage MOFs.^[17] Very recently, solid state NMR and molecular simulations were used to distinguish (on average) between alternating, random, and cluster ligand distribution in MixMOFs isorecticular to MOF-5.^[18] This indirect approach is certainly a step forward in the characterization of MixMOFs but does not provide spatial information for the ligand distribution within a crystal. The PTIR technique is applied here to overcome these limitations and determine the nanoscale linker heterogeneity in amino-containing bifunctional MOF crystals.

In PTIR, also known as AFM-IR, the sample is placed on an optical prism and illuminated by total internal reflection with a pulsed tunable IR laser, while a contact AFM tip extracts the local chemical composition (Figure 1). Our PTIR set up uses two pulsed laser sources tunable between 1.55 μm (6650

cm⁻¹) and 16.00 μm (625 cm⁻¹). The absorption of a laser pulse in the sample results in local heating, sample expansion, and excitation of the AFM cantilever motion, which is monitored by a four-quadrant photodetector. The local IR spectrum is obtained by plotting the maximum amplitude of the cantilever deflection as a function of the wavelength. PTIR chemical maps are obtained by illuminating the sample at a fixed wavelength while scanning the AFM tip. The typical laser spot size is ≈ 30 μm, but the AFM tip acts as a “spatial filter” allowing the extraction of spectroscopic information with nanoscale resolution,^[13b] several times smaller than the diffraction limit of IR light. Since the PTIR signal is proportional to the absorbed energy,^[13b] PTIR spectra can be used for material identification by comparison with IR spectral libraries.^[19] For thin samples (<1 μm) the PTIR signal increases linearly with sample thickness^[13b] while the sensing mechanism (probe actuation), makes samples with large linear expansion coefficients (α) like polymers^[13b, 20] or biological samples^[13a, 21] easier to measure. This work demonstrates that MOFs, which typically have relatively small and negative α ,^[22] are also amenable to PTIR characterization.

The structure of MIL-68 exhibits a rod-shaped structure, formed by indium octahedra and terephthalates as bridging linkers^[14] resulting in hexahedral and triangular 1D-channels with apertures of 1.6 nm and 0.6 nm respectively (Figure 1 inset). The samples contain pure bdc or abdc linker or a mixture of them obtained either solvothermally from a solution or by post-synthetic ligand exchange.^[23] Depending on synthetic conditions, homogeneous or gradient compositions can be obtained (see below). Homolinker samples of In-MIL-68 (**I**, bdc linker) and In-MIL-68-NH₂ (**II**, abdc linker) were synthesized according to literature and used as references.^[14, 24] Three mixed-linker In-MIL-68 samples made from bdc and abdc were synthesized by different methods (summarized in Table 1) The crystallization from a solution containing an equal concentration of bdc and abdc linkers yields rod shaped crystals tens of microns in length of corresponding composition (sample **III**). Similarly to published methods of post-synthetic ligand exchange,^[23c] placing In-MIL-68 seed rods in a solution containing abdc at 100 °C for 48 hr yields a material with an average linker composition of bdc:abdc = 2:1 for **IV**.

To achieve ligand anisotropy within the In-MIL-68 isoreticular structure, a spatially confined, *in situ* sequential synthesis was devised, using conditions similar to those reported previously.^[24a] The confinement allows monitoring the growth *in situ* with an optical microscope and it suppresses seeded vertical growth of the crystals, which could complicate PTIR characterization. In-MIL-68 seed crystals were grown directly on the ZnSe prism under 2D physical confinement. Two solutions of indium and desired linker were sequentially added and heated; the initial In-MIL-68 crystals acted as a seed for the secondary growth of In-MIL-68-NH₂ (**V**). All samples (**I** to **V**) were characterized with PTIR to determine the distribution of organic linkers in the MOF framework. In a typical experiment (for **I** to **IV**), a dilute methanolic suspension prepared from activated MOF powder was cast on a ZnSe prism and

allowed to dry before the PTIR measurement. After recording the AFM height image, the AFM tip is moved to various locations on the crystal and PTIR spectra are collected at each location.

Representative PTIR spectra of monoligand MOF samples **I** and **II** show common and distinctive absorption peaks (Figure 2). The C-H out of plane bending frequencies (around 700 cm^{-1}) are widely used in IR spectroscopy to identify the position and number of chemical substitutions in aromatic rings.^[25] Not surprisingly the two MOFs show distinct peaks in this region, 742 cm^{-1} for **I** and 762 cm^{-1} for **II**. A peak at 1260 cm^{-1} , characteristic of the C-N stretching, is observed in the spectrum of **II** which is of course absent in **I**. The peaks at 1390 cm^{-1} and 1556 cm^{-1} , assigned to the symmetric and antisymmetric carboxylate stretching,^[24a] prove that the ligands are part of the framework and are not just adsorbates. This conclusion is supported by the absence of a peak at $\approx 1672\text{ cm}^{-1}$, characteristic of uncoordinated carboxylic groups in these ligands (Figure 2, S4 and S5).

The spectra of sample **III** resemble a combination of the two homoligand MOFs' spectra (Figure 2). PTIR spectra collected near the center, near the tip, and on the tip of a crystal of **III** are essentially identical, indicating ligand homogeneity (Figure 3).

The PTIR spectra of the ligand-exchanged sample **IV** resemble the spectra of **III** (Figure 2). Chemical maps (Figure S6) of crystals of **IV** also show homogeneity of linker distribution. We believe that the ligand homogeneity in these samples results from the ease of ligand exchange in MOFs isoreticular to In-MIL-68.^[23b] Our data suggest that ligand exchange occurs homogeneously through the crystals under the synthetic conditions used here. PTIR spectra from all samples compare favourably with those taken at the macroscale with a FTIR spectrometer (Figure S4).

The growth of **V** was monitored *in situ* with an optical microscope (Figure S7). During the secondary growth the crystals grew several microns in the direction of the long, c-axis and minimally in width. The same crystals were easily located using an optical microscope integrated with the PTIR set-up. PTIR spectra (Figure 2) reveal that both ligands are present throughout these crystals, suggesting that some ligand exchange takes place in the seed crystal (Figure S8). However, chemical maps of **V** reveal a lengthwise heterogeneous distribution of ligands (Figure 4).

Two crystals of **V** identified by arrows in Figure S7 were imaged: one in its entirety at moderate spatial resolution (Figure 4 a-c) and one near the tip at high resolution (Figure 4 d-f). The insets in Figure 4 show the PTIR intensity profiles over the long axis of the MOF crystals. The maps of the abdc C-N stretch at 1260 cm^{-1} (Figure 4 b,e) show stronger intensity at the crystal ends, indicating that the material grown on the seed crystals is richer in the aminated ligand as compared to the seed. Chemical maps of the common carboxylate stretching frequencies (Figure 4 c,f) shows the expected uniformity of this moiety and confirms (along with no measureable peak at 1672 cm^{-1}) that the abdc ligand comprises the framework. The high (100 nm) resolution C-N stretch map reveals a fairly abrupt concentration gradient; occurring

within ≈ 600 nm (Figure 4e). In contrast, the map of the common antisymmetric carboxylate stretch shows no gradient (Figure 4f).

In conclusion a novel, *in situ* process for engineering submicron linker anisotropy in MixMOFs is presented here. The PTIR technique enables imaging heterogeneous and homogeneous domains in MOF single crystallites with nanoscale resolution and enables determining the extent of linker gradients between MOF domains. Additionally, the linker homogeneity of In-MIL-68 MixMOFs, obtained from direct crystallization and post-synthetic linker exchange is proved unambiguously, as postulated in previous reports.^[23] This find is of particular relevance because uniform distribution of active sites is a prerequisite for preparing efficient catalysts and sensors. Such proof together with the MOF extended and ordered molecular structure reinforce the belief that MOFs may be used as model catalyst materials whose active sites may, in principle, be characterized as completely as those of molecular species. We believe that the proof of concepts presented here will foster mixed-MOF research, leading to better understanding of these materials and consequently help engineer them for greatest efficacy.

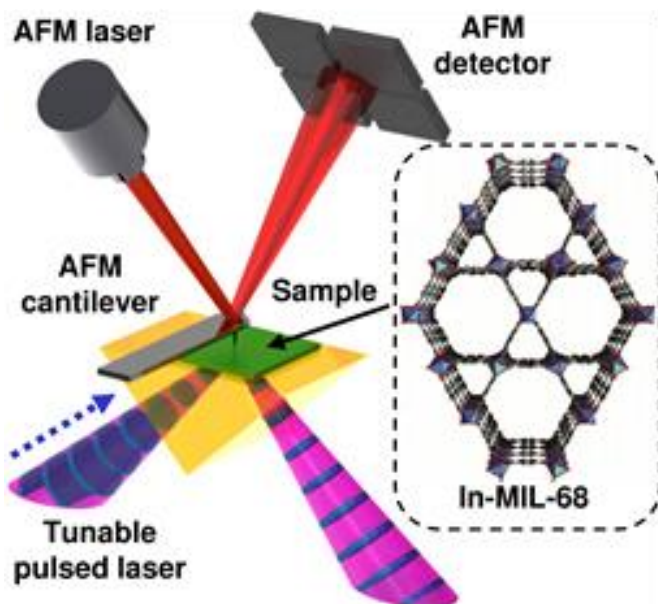


Figure 1. PTIR Schematic: The IR laser beam (envelope in pink) illuminates the sample via total internal reflection. The absorption in the sample results in thermal expansion and deflection of the AFM cantilever. The inset depicts the crystal structure of In-MIL-68.

Table 1. Preparation of MIL-68 samples^[a]

Synthesis method	sample	Linker composition ^[b]
crystallization from solution	I	bdc
crystallization from solution	II	abdc
crystallization from solution	III	bdc:abdc = 1:1
post-synthetic exchange	IV	bdc:abdc = 2:1
sequential growth	V	not determined

[a] All synthesis details are reported in the supporting information; [b] Determined by liquid state ¹H NMR of a dissolved MOF sample.

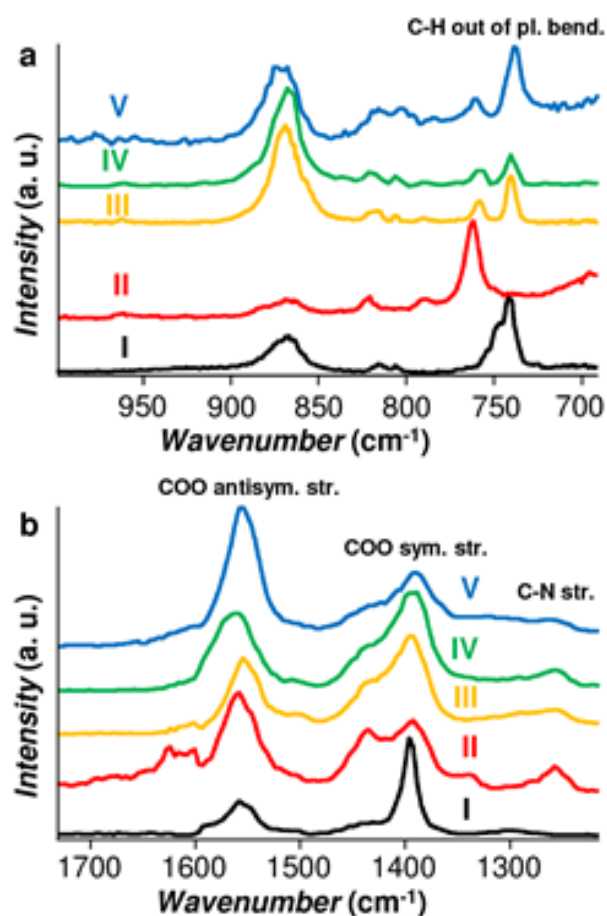


Figure 2. (a,b) Representative FTIR spectra for MIL-68 samples I to V. The spectra are displayed with an offset for clarity.

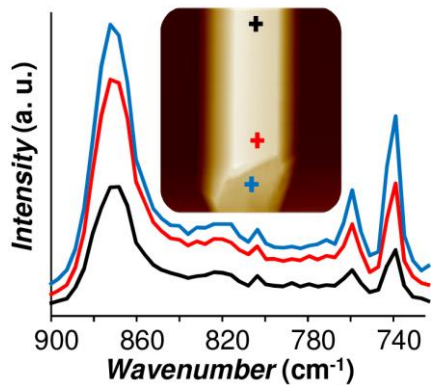


Figure 3. PTIR spectra of III taken at the color-coded locations denoted in AFM height image (inset). The spectra are displayed with an offset for clarity.

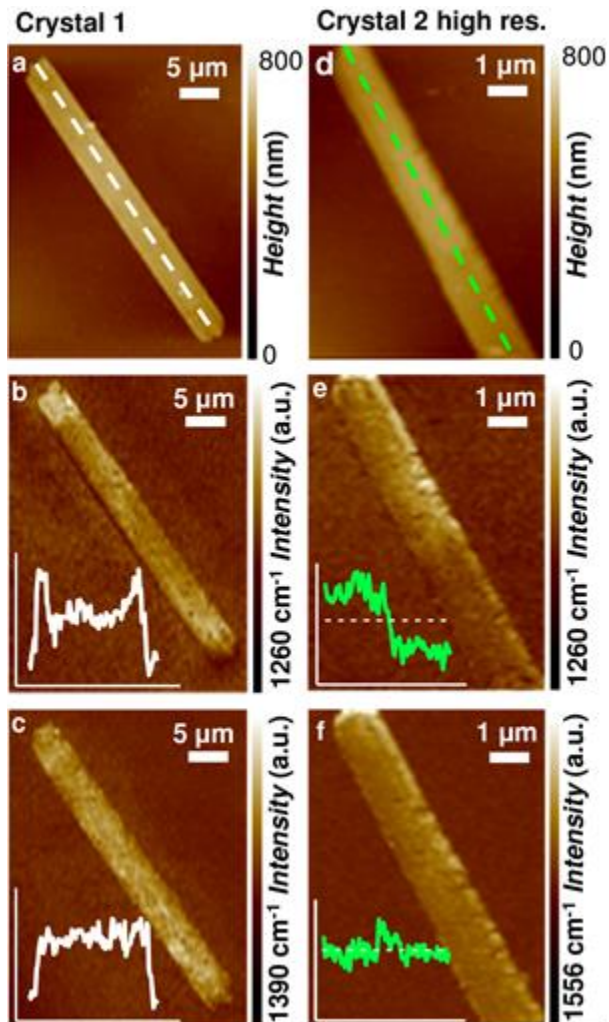


Figure 4. (a) Moderate resolution AFM height image, (b) PTIR map of the C-N stretch and (c) PTIR map of the common symmetric carboxylate stretch for the crystal designated by the white arrow in Figure S7. (d) High resolution AFM height image, (e) PTIR map of the C-N stretch and (f) PTIR map of the common antisymmetric carboxylate stretch for the crystal designated by the green arrow in Figure S7. Insets are PTIR intensity profiles along the crystal's long axis indicated by the dashed lines in the height images. The dashed lines of (e,f) are to guide only.

Keywords: PTIR · Metal-Organic Framework · MixMOF · Infrared Spectroscopy · Nanoscale Chemical Imaging

- [1] a) M. Eddaoudi, J. Kim, N. Rosi, D. Vodak, J. Wachter, M. O'Keeffe, O. M. Yaghi, *Science* **2002**, 295, 469-472; b) L. Ma, J. M. Falkowski, C. Abney, W. Lin, *Nat. Chem.* **2010**, 2, 838-846.
- [2] a) L. Alaerts, M. Maes, L. Giebeler, P. A. Jacobs, J. A. Martens, J. F. M. Denayer, C. E. A. Kirschhock, D. E. De Vos, *J. Am. Chem. Soc.* **2008**, 130, 14170-14178; b) A. Centrone, E. E. Santiso, T. A. Hatton, *Small* **2011**, 7, 2356-2364.
- [3] S. K. Henninger, H. A. Habib, C. Janiak, *J. Am. Chem. Soc.* **2009**, 131, 2776-2777.
- [4] a) W. Kleist, M. Maciejewski, A. Baiker, *Thermochim. Acta* **2010**, 499, 71-78; b) J. Lee, O. K. Farha, J. Roberts, K. A. Scheidt, S. T. Nguyen, J. T. Hupp, *Chem. Soc. Rev.* **2009**, 38, 1450-1459.
- [5] a) A. Fateeva, P. A. Chater, C. P. Ireland, A. A. Tahir, Y. Z. Khimiyak, P. V. Wiper, J. R. Darwent, M. J. Rosseinsky, *Angew. Chem. Int. Ed.* **2012**, 51, 7440-7444; b) Y. Fu, D. Sun, Y. Chen, R. Huang, Z. Ding, X. Fu, Z. Li, *Angew. Chem. Int. Ed.* **2012**, 51, 3364-3367; c) P. Wu, C. He, J. Wang, X. Peng, X. Li, Y. An, C. Duan, *J. Am. Chem. Soc.* **2012**, 134, 14991-14999; d) M. Dan-Hardi, C. Serre, T. Frot, L. Rozes, G. Maurin, C. Sanchez, G. Ferey, *J. Am. Chem. Soc.* **2009**, 131, 10857-10858.
- [6] H. Deng, C. J. Doonan, H. Furukawa, R. B. Ferreira, J. Towne, C. B. Knobler, B. Wang, O. M. Yaghi, *Science* **2010**, 327, 846-850.
- [7] P. Horcajada, et al., *Nat. Mater.* **2010**, 9, 172-178.
- [8] L. E. Kreno, K. Leong, O. K. Farha, M. Allendorf, R. P. Van Duyne, J. T. Hupp, *Chem. Rev.* **2012**, 112, 1105-1125.
- [9] a) W. Xuan, C. Zhu, Y. Liu, Y. Cui, *Chem. Soc. Rev.* **2012**, 41, 1677-1695; b) J. Della Rocca, D. Liu, W. Lin, *Acc. Chem. Res.* **2011**, 44, 957-968.
- [10] a) S. Furukawa, et al., *Angew. Chem.* **2009**, 48, 1766-1770; b) X. Song, T. K. Kim, H. Kim, D. Kim, S. Jeong, H. R. Moon, M. S. Lah, *Chem. Mater.* **2012**, 24, 3065-3073; c) K. Koh, A. G. Wong-Foy, A. J. Matzger, *Chem. Commun.* **2009**, 6162-6164.
- [11] a) S. Marx, W. Kleist, J. Huang, M. Maciejewski, A. Baiker, *Dalton Trans.* **2010**, 39, 3795-3798; b) A. A. Talin, et al., *Science* **2014**, 343, 66-69.
- [12] U. Díaz, M. Boronat, A. Corma, *Proc. R. Soc. A.* **2012**, 468, 1927-1954.
- [13] a) A. Dazzi, R. Prazeres, F. Glotin, J. M. Ortega, M. Al-Sawaftah, M. de Frutos, *Ultramicroscopy* **2008**, 108, 635-641; b) B. Lahiri, G. Holland, A. Centrone, *Small* **2013**, 9, 439-445; c) B. Lahiri, G. Holland, V. Aksyuk, A. Centrone, *Nano Lett.* **2013**, 13, 3218-3224; d) A. M. Katzenmeyer, V. Aksyuk, A. Centrone, *Anal. Chem.* **2013**, 85, 1972-1979; e) J. R. Felts, K. Kjolter, M. Lo, C. B. Prater, W. P. King, *ACS Nano* **2012**, 6, 8015-8021; f) A. Dazzi, F. Glotin, R. Carminati, *J. Appl. Phys.* **2010**, 107, -; g) A. Dazzi, R. Prazeres, F. Glotin, J. M. Ortega, *Infrared Phys. Technol.* **2006**, 49, 113-121.
- [14] C. Volkringer, M. Meddouri, T. Loiseau, N. Guillou, J. Marrot, G. Ferey, M. Haouas, F. Taulelle, N. Audebrand, M. Latroche, *Inorg. Chem.* **2008**, 47, 11892-11901.
- [15] S. Furukawa, K. Hirai, Y. Takashima, K. Nakagawa, M. Kondo, T. Tsuruoka, O. Sakata, S. Kitagawa, *Chem. Commun.* **2009**, 5097-5099.
- [16] T. Fukushima, S. Horike, H. Kobayashi, M. Tsujimoto, S. Isoda, M. L. Foo, Y. Kubota, M. Takata, S. Kitagawa, *J. Am. Chem. Soc.* **2012**, 134, 13341-13347.
- [17] R. J. T. Houk, B. W. Jacobs, F. E. Gabaly, N. N. Chang, A. A. Talin, D. D. Graham, S. D. House, I. M. Robertson, M. D. Allendorf, *Nano Lett.* **2009**, 9, 3413-3418.

- [18] X. Kong, H. Deng, F. Yan, J. Kim, J. A. Swisher, B. Smit, O. M. Yaghi, J. A. Reimer, *Science* **2013**, *341*, 882-885.
- [19] C. Marcott, M. Lo, K. Kjoller, C. Prater, I. Noda, *Appl. Spectrosc.* **2011**, *65*, 1145-1150.
- [20] B. Van Eerdenbrugh, M. Lo, K. Kjoller, C. Marcott, L. S. Taylor, *Mol. Pharm.* **2012**, *9*, 1459-1469.
- [21] C. Policar, J. B. Waern, M.-A. Plamont, S. Clède, C. Mayet, R. Prazeres, J.-M. Ortega, A. Vessières, A. Dazzi, *Angew. Chem. Int. Ed.* **2011**, *50*, 860-864.
- [22] D. Dubbeldam, K. S. Walton, D. E. Ellis, R. Q. Snurr, *Angew. Chem. Int. Ed.* **2007**, *46*, 4496-4499.
- [23] a) A. F. Gross, E. Sherman, S. L. Mahoney, J. J. Vajo, *J. Phys. Chem. A* **2013**, *117*, 3771-3776; b) M. Kim, J. F. Cahill, H. Fei, K. A. Prather, S. M. Cohen, *J. Am. Chem. Soc.* **2012**, *134*, 18082-18088; c) M. Kim, J. F. Cahill, Y. Su, K. A. Prather, S. M. Cohen, *Chem. Sci.* **2012**, *3*, 126-130; d) T. Li, M. T. Kozlowski, E. A. Doud, M. N. Blakely, N. L. Rosi, *J. Am. Chem. Soc.* **2013**, *135*, 11688-11691.
- [24] a) L. Wu, M. Xue, S.-L. Qiu, G. Chaplais, A. Simon-Masseron, J. Patarin, *Microporous Mesoporous Mater.* **2012**, *157*, 75-81; b) M. Savonnet, D. Bazer-Bachi, N. Bats, J. Perez-Pellitero, E. Jeanneau, V. Lecocq, C. Pinel, D. Farrusseng, *J. Am. Chem. Soc.* **2010**, *132*, 4518-4519.
- [25] R. N. Jones, C. Sandorfy, in *Technique of Organic Chemistry*, Vol. IX (Ed: A. Weissberger), Interscience, New York, **1956**.

Supporting Information

Additional Experimental information

1. Materials synthesis	11
2. FTIR spectroscopy	15
3. PTIR experimental	16
4. PTIR supplemental discussion.....	17
5. Additional PTIR data.....	18
6. Additional References.....	21

1. Materials synthesis

All reactions were carried out in anhydrous solvents. All other reagents are commercially available and were used without further purification. NMR spectra were recorded on a 250 MHz spectrometer. Chemical shifts are reported in parts per million (HZ/MHz) referenced to the appropriate solvent peak. The XRD measurements (figure S1) on the materials are carried out by powder X-ray diffraction (PXRD) using a diffractometer equipped with a secondary graphite monochromator and a scintillation counter.

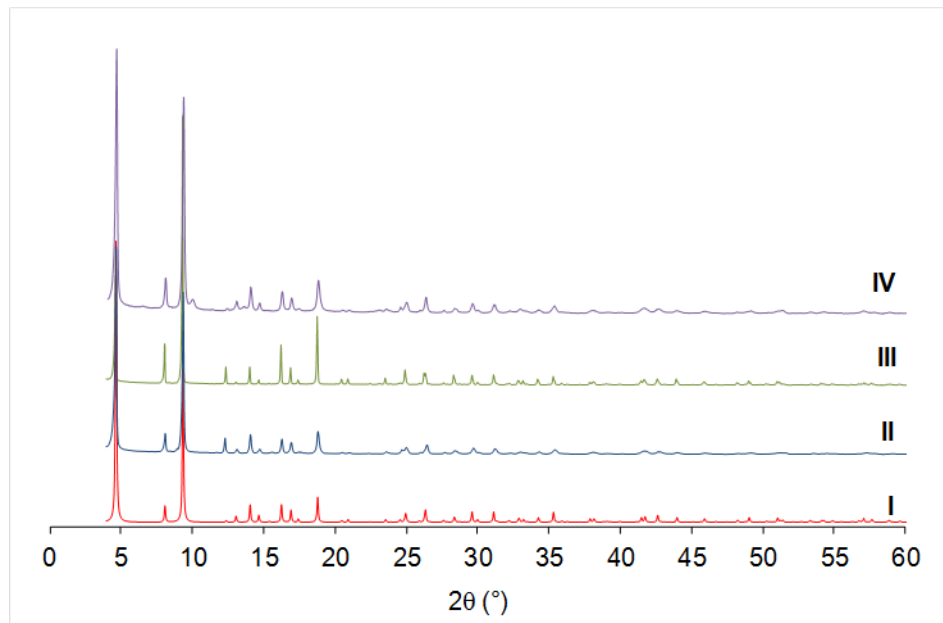


Figure S1. PXRD patterns of MIL-68 samples **I** to **IV** (from bottom to top).

1.1 Self-assembled materials **I** to **III**

In-MIL-68 was synthesized and activated according to our previously reported procedure.^[24b, 26] In a typical solvothermal synthesis, indium nitrate hydrate (408 mg) and terephthalic acid (bdc, 200 mg) are dissolved in 5 mL of dimethylformamide (DMF). The solution is placed in an autoclave equipped with a polytetrafluoroethylene liner at 373 K for 48 hr.

The crystalline powder is then collected by centrifugation and washed three times with 7 mL of DMF at room temperature. The solid is finally washed with a soxhlet using dichloromethane and dried under vacuum at room temperature to afford In-MIL-68 (**I**) as a white crystalline powder.

Compounds **II** and **III** are similarly obtained using 2-aminoterephthalic acid (abdc, 175 mg) for **II**, and a mixture of terephthalic acid (bdc, 100 mg) and 2-aminoterephthalic acid (87 mg) for **III**. According to ¹H NMR analysis of a sample of **III** digested in an acidic solution of DCl-D₂O in DMSO-d₆, the ligand ratio in **III** is bdc : abdc = 1 ± 0.1 : 1 ± 0.1 as determined by the integration of the NMR lines (Figure S2). The uncertainties are single standard deviations in the integration of the NMR lines.

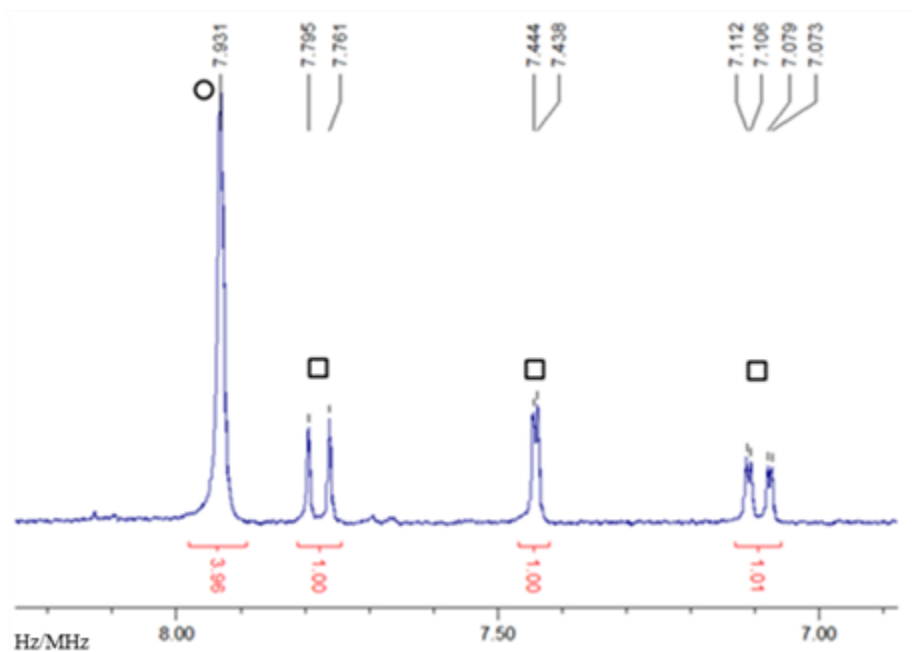


Figure S2. ^1H NMR spectra of **III** digested in $\text{DCI-D}_2\text{O/dmsO-d}_6$. Proton signals from bdc and abdc are indicated by circle and squares respectively.

1.2 Post-synthetic ligand exchange (**IV**)

A sample of In-MIL-68 (**I**, 80 mg) prepared as described above is suspended in a solution of 2-aminoterephthalic acid (10 mg) in 5 mL of DMF. The suspension is placed in an autoclave equipped with a polytetrafluoroethylene liner at 373 K for 48 hours.

The crystalline powder is then collected by centrifugation and washed three times with 7 mL of DMF at room temperature. The solid is finally washed with a soxhlet using dichloromethane and dried under vacuum at room temperature to afford **IV** as an off-white crystalline powder. According to ^1H NMR analysis of a sample of **IV** digested in an acidic solution of $\text{DCI-D}_2\text{O}$ in DMSO-d_6 , the ligand ratio in **IV** is $\text{bdc} : \text{abdc} = 2 \pm 0.2 : 1 \pm 0.1$ as determined by the integration of the NMR lines (Figure S3). The uncertainties are single standard deviations in the integration of the NMR lines.

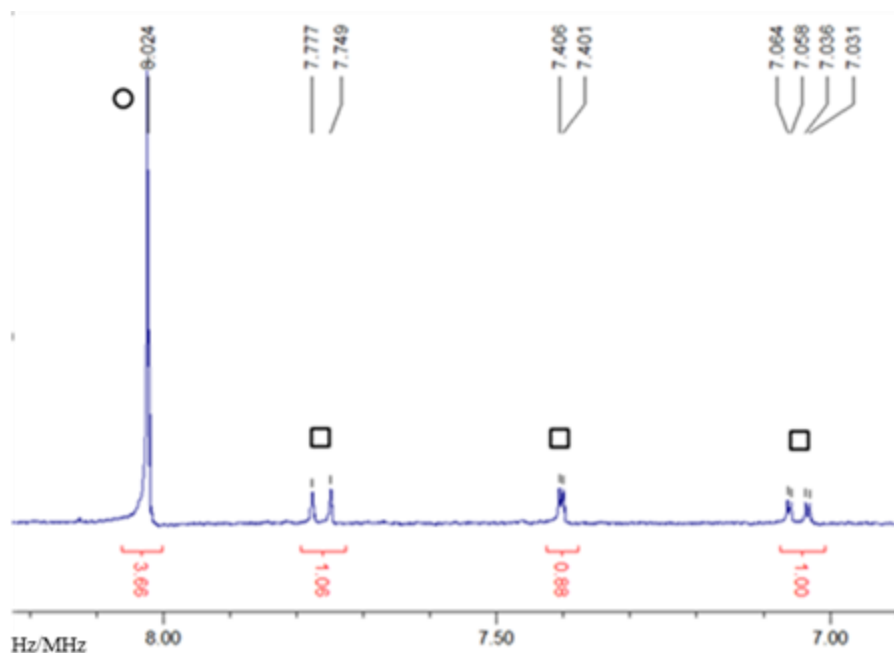


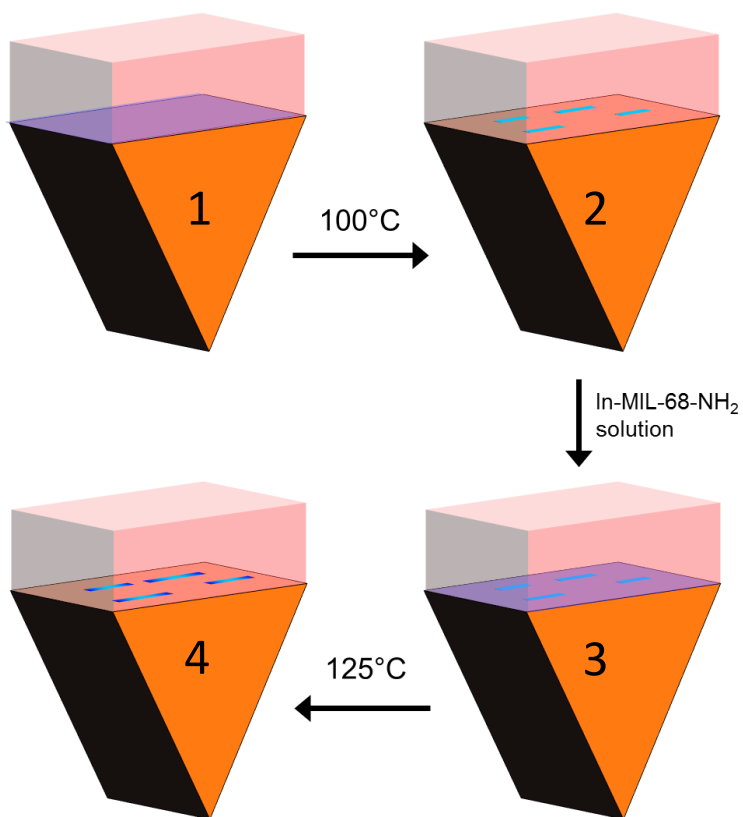
Figure S3. ^1H NMR spectra of **IV** digested in $\text{DCl-D}_2\text{O/dmsO-d}_6$. Protons signals from *bdc* and *abdc* are indicated by circle and squares respectively.

1.3 *In situ* confined synthesis of compound **V**

In-MIL-68 precursor solution was prepared according to prior reports.^[14, 24a] *bdc* (0.0455 g) in DMF (1.25 mL) was sonicated until fully dissolved. In(III) nitrate hydrate (0.1075 g) was then added and sonicated until fully dissolved. In-MIL-68-NH₂ precursor solution was prepared according to ^[24a]. *abdc* (0.0246 g) was sonicated in DMF (1.25 mL) until fully dissolved. Subsequently In(III) nitrate hydrate (0.134 g) was added and sonicated until fully dissolved.

In-MIL-68 seed crystals were grown directly on the ZnSe prism under 2D physical confinement. Scheme 1 depicts the process. The numbering in the following description refers to the step in the scheme. The prism and a smooth glass coverslip were washed with a commercial detergent and warm water, rinsed with warm water, and blown dry with nitrogen. A small drop ($\ll 1\mu\text{L}$) of precursor solution was dispensed onto the prism and pressed manually with the coverslip (**1**). Appropriate thinness of the solution film (i.e. submicron) is apparent by the formation of Newton ring-like interference patterns. Coverslips used were of appropriate smoothness for anodic bonding. The prism was placed in a custom-made holder to provide appropriate orientation and facilitate thermal contact to the heated stage. The holder was immobilized on the stage via vacuum. The stage was resistively heated using a variable transformer and the temperature monitored by type K thermocouple. Temperature calibration, as a function of transformer setting, was performed before the synthesis. Temperature uncertainty was determined to ± 5 K in the range of temperature used. The sample was heated to 373 K leading to the formation of rod shaped crystals typical of In-MIL-68, until most of the solvent evaporated (**2**). After

cooling the sample, a droplet of In-MIL-68-NH₂ precursor solution was introduced by capillarity without disturbing the coverslip (**3**). The sample was then heated to 398 K (**4**) and monitored with an optical microscope. After completing the synthesis, the coverslip was removed and the sample (**V**) was rinsed thoroughly with DMF, blown dry with nitrogen, and finally heated (398 K, 10 min) to evacuate any remaining solvent. The microscope used to monitor growth was fitted with a 20X, 0.42 N.A. long working-distance objective and a digital camera.



Scheme 1. *In situ* synthesis of MOFs with anisotropic ligand distribution.

2. FTIR spectroscopy

Fourier Transform Infrared (FTIR) spectra of MOF powder samples were recorded with an FTIR spectrometer equipped with an attenuated total reflection (ATR) accessory. 128 spectra (2 cm^{-1} resolution) were acquired and averaged for each sample.

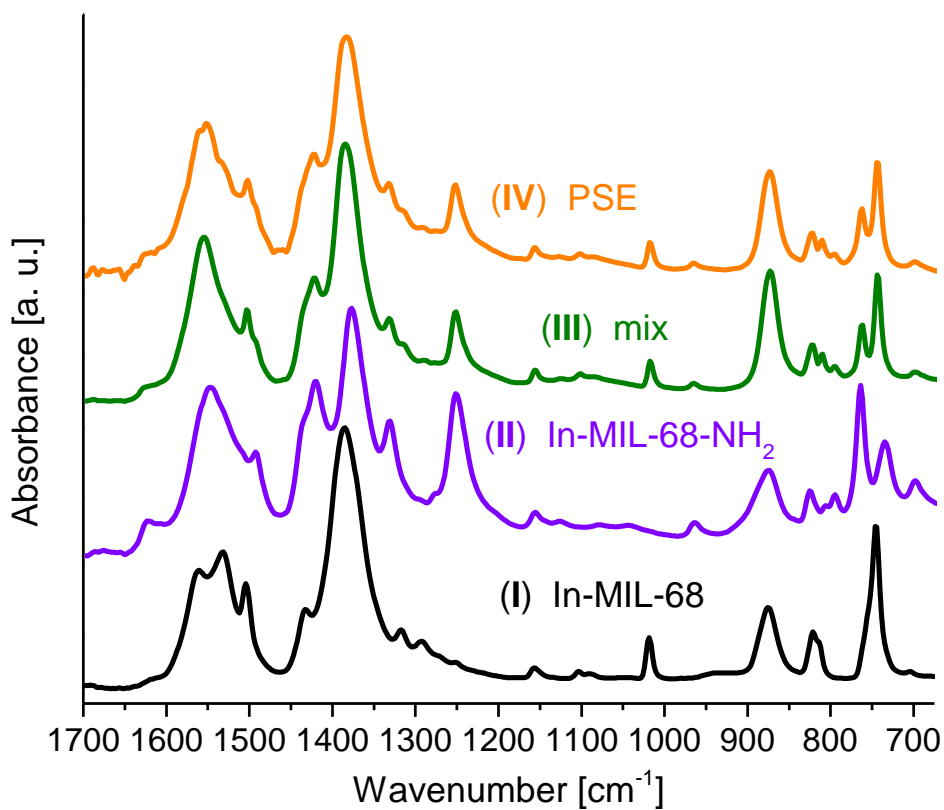


Figure S4. FTIR spectra of In-MIL-68 (I), In-MIL-68-NH₂ (II), mix-MOF prepared using equal amount of bdc:abdc ligands (III), and of (IV) (where crystals of I were added to a solution of abdc).

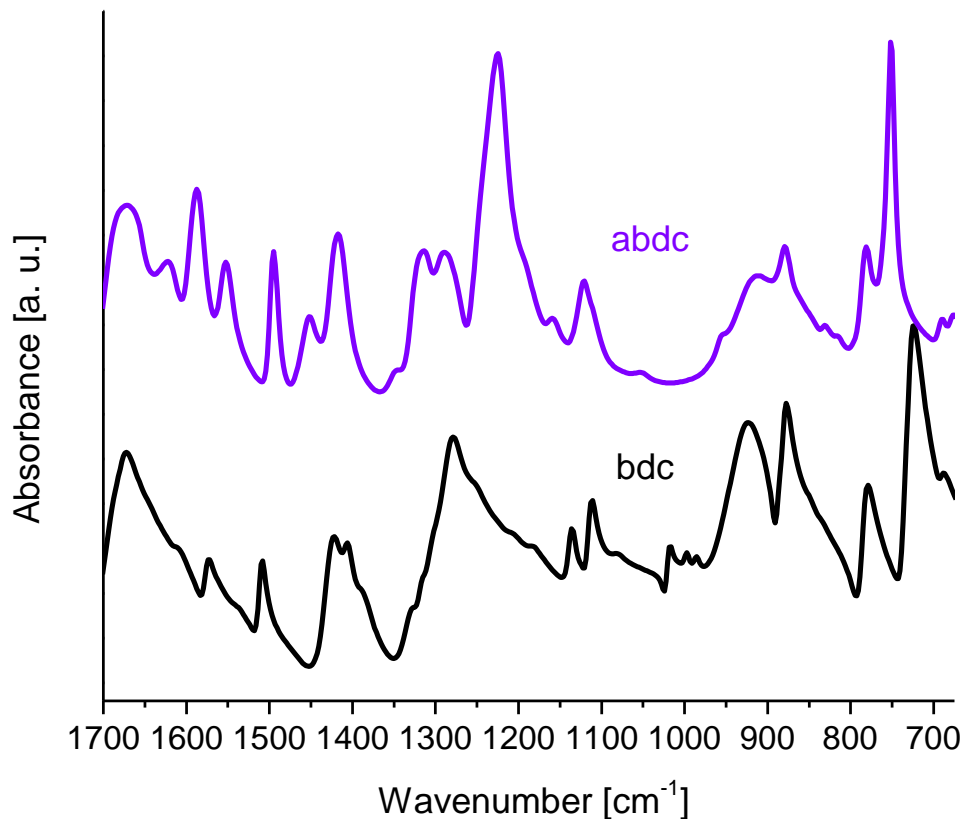


Figure S5. FTIR spectra of free bdc and abdc linkers.

3. PTIR experimental

PTIR experiments were carried out using a modified commercial PTIR setup^[13d] which consists of an AFM microscope operating in contact mode and two tunable pulsed laser sources covering the spectral range between 1.55 μm and 16.00 μm (from 6650 cm^{-1} to 625 cm^{-1}). The laser light (1 μJ and 5 μJ per pulse) was focused under the AFM tip with a ZnSe lens to a spot of 30 $\mu\text{m} \pm 10 \mu\text{m}$ in diameter. The AFM tip acts as a spatial filter allowing the extraction of spectroscopic information with nanoscale resolution. The low repetition rate of the laser (1 kHz) assures that a new pulse will excite the sample and cantilever only after they have returned to equilibrium. PTIR spectra were recorded by tuning the laser(s) at intervals of 2 cm^{-1} or 4 cm^{-1} and co-averaging ring-down intensity from 256 laser pulses at each wavelength. Chemical maps (collected synchronously with AFM height images)^[13b] are comprised of pixels 100 nm x 100 nm with the exception of figure 3a-c where the pixel resolution is 300 nm x 533 nm. Pixel intensity represents average PTIR signal for 32-128 laser pulses. Line intensity profiles of chemical maps represent the average of 3-6 pixels perpendicular to the long axis of the rod. PTIR resolution well below 100 nm has been reported previously.^[27] Here we estimate the resolution to be limited by the pixel size (100 nm). Commercially available 205 μm long silicon nitride contact-mode AFM probes with a nominal spring constant between 0.03 N/m and 0.12 N/m were used throughout this study.

4. PTIR supplemental discussion

Although the structure of MIL-68 is anisotropic, we did not observe any difference in PTIR lateral resolution in the direction parallel or perpendicular to the crystal *c* axis. Differences in thermal conductivity as a function of the crystallographic direction could in principle influence the PTIR lateral resolution^[13a]; such effect is expected to be very weak because of the low thermal conductivity of MOF materials.^[28]

Light polarization was fixed in the experiments reported here. We note that for a crystalline material in which an IR active dipole occurs for each unit cell in a particular crystallographic direction, the IR light absorption intensity is maximum when the dipole and the IR light's linear polarization are parallel. However, in the mix-In-MIL-68 crystals studied here, the electric dipoles associated with the ligand-specific vibrational modes (C-H out of plane bending and C-N stretching) are randomly distributed through the crystals due to torsional disorder of the linkers' aromatic unit in the structure because of the multiple directions in which the linkers are assembled in the MOFs (see figure 1 inset). Consequently no differences in the peak intensity as a function of crystal orientation are observed in the MOF for those chemically-diagnostic peaks. On the contrary, the symmetric and antisymmetric carboxylic stretching dipoles (common to both *bdc* and *abdc*) are orthogonal to one another, and their relative intensity depends on the crystal orientation with respect to light polarization direction. The relative intensity differences amongst these peaks in figure 2b are the result of differences in crystal orientation.

5. Additional PTIR data

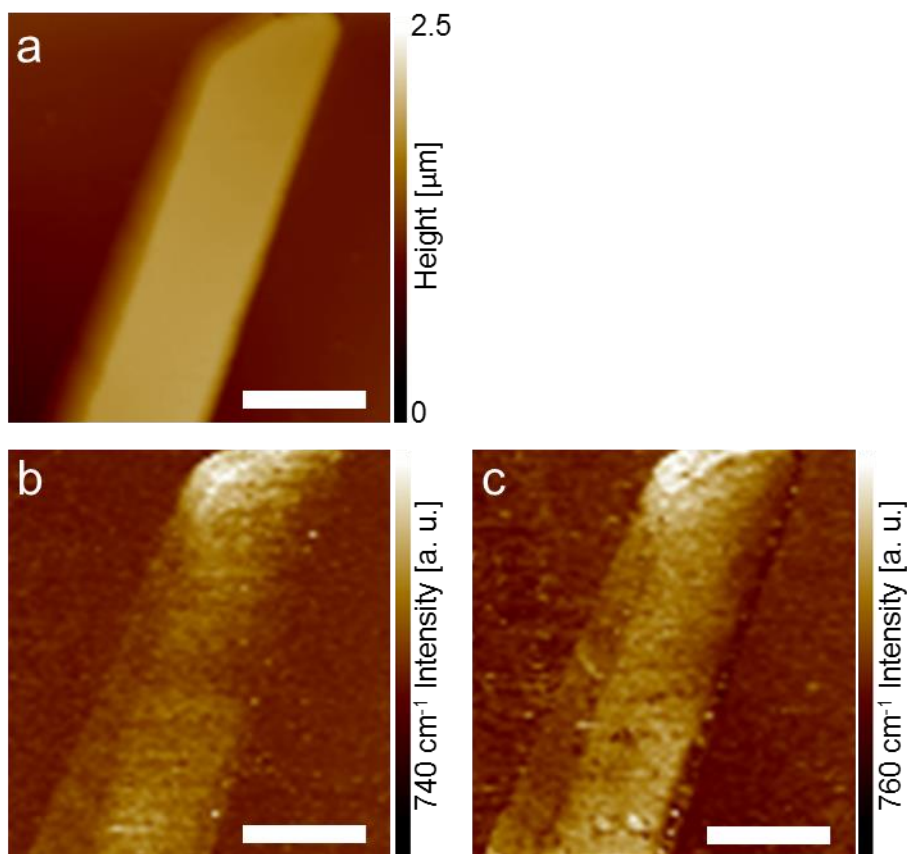


Figure S6. a) AFM height image of MOF crystal from sample IV. b) Corresponding PTIR chemical map obtained by illuminating the sample at 740 cm^{-1} , characteristic of the bdc ligand of In-MIL-68. c) Corresponding PTIR chemical map obtained by illuminating the sample at 760 cm^{-1} , characteristic of the abdc ligand of In-MIL-68-NH₂. Similar to what was observed for III (see Figure 3), we do not see any clear evidence of ligand inhomogeneity despite the ability to interrogate the MOF crystal composition at any location. Note that in figure S6b and S6c there are relatively brighter and darker spots, however these are common to the two chemically anti-correlated peaks and are therefore *not* indicative of ligand anisotropy. Scale bars are $2.5\text{ }\mu\text{m}$.

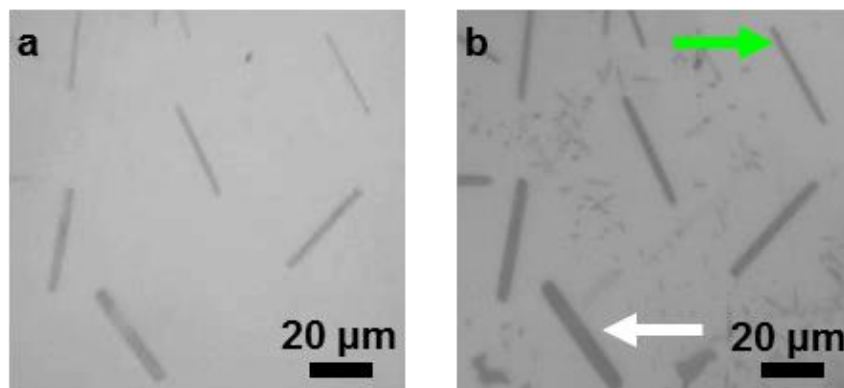


Figure S7. Optical Images showing the growth of **V** from In-MIL-68 seed crystals in In-MIL-68-NH₂ precursor solution at beginning (a) and end (b) of seeded growth. The crystals designated by the white and green arrows in panel b were characterized with the PTIR technique in figure 4a-c and 4d-f, respectively.

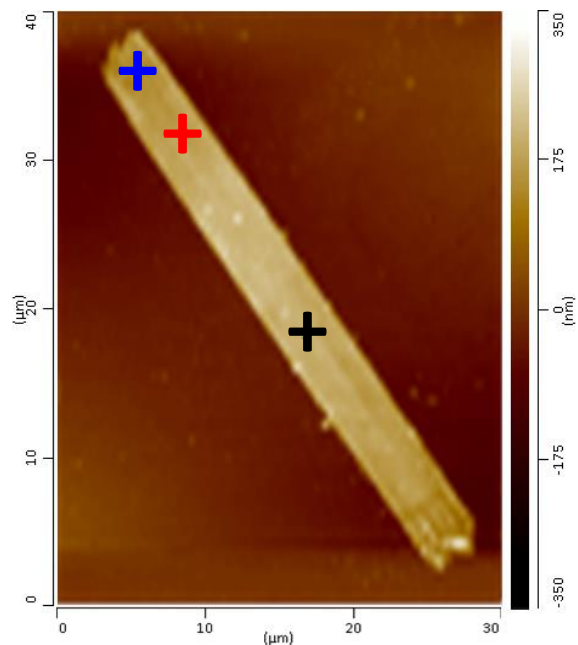
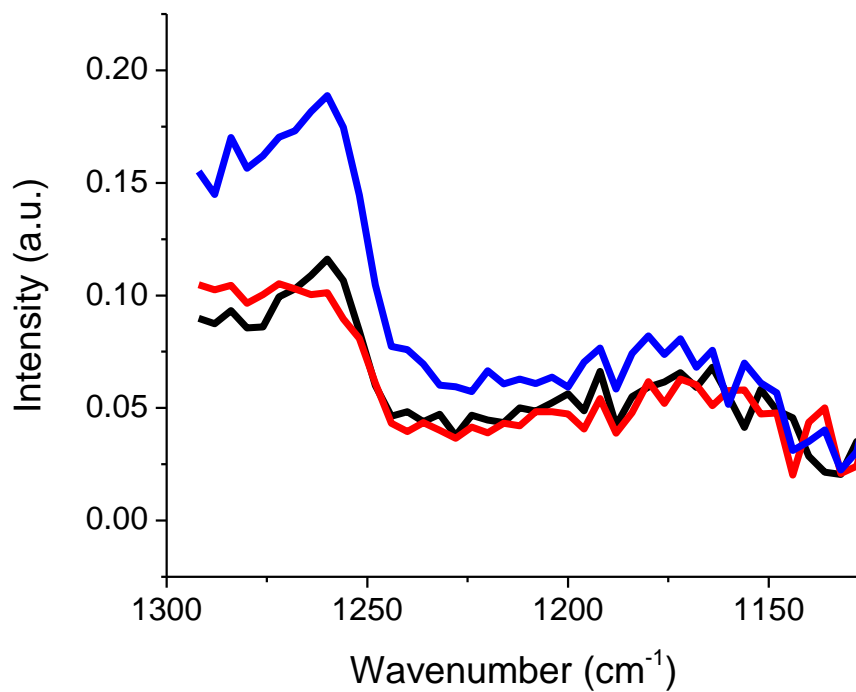


Figure S8. Spectra in the C-N stretching (1260 cm^{-1}) region recorded at the corresponding color-coded locations on the height image for the crystal denoted by the white arrow in figure S7 and mapped in figure 4a-c. The signal to noise ratio observed for such thin structures is improved by increased averaging. Each spectrum is the average of two spectra taken at the given location using the parameters discussed above.

6. Additional References

- [1] aM. Eddaoudi, J. Kim, N. Rosi, D. Vodak, J. Wachter, M. O'Keeffe, O. M. Yaghi, *Science* **2002**, *295*, 469-472; bL. Ma, J. M. Falkowski, C. Abney, W. Lin, *Nat. Chem.* **2010**, *2*, 838-846.
- [2] aL. Alaerts, M. Maes, L. Giebeler, P. A. Jacobs, J. A. Martens, J. F. M. Denayer, C. E. A. Kirschhock, D. E. De Vos, *J. Am. Chem. Soc.* **2008**, *130*, 14170-14178; bA. Centrone, E. E. Santiso, T. A. Hatton, *Small* **2011**, *7*, 2356-2364.
- [3] S. K. Henninger, H. A. Habib, C. Janiak, *J. Am. Chem. Soc.* **2009**, *131*, 2776-2777.
- [4] aW. Kleist, M. Maciejewski, A. Baiker, *Thermochim. Acta* **2010**, *499*, 71-78; bJ. Lee, O. K. Farha, J. Roberts, K. A. Scheidt, S. T. Nguyen, J. T. Hupp, *Chem. Soc. Rev.* **2009**, *38*, 1450-1459.
- [5] aA. Fateeva, P. A. Chater, C. P. Ireland, A. A. Tahir, Y. Z. Khimiyak, P. V. Wiper, J. R. Darwent, M. J. Rosseinsky, *Angew. Chem. Int. Ed.* **2012**, *51*, 7440-7444; bY. Fu, D. Sun, Y. Chen, R. Huang, Z. Ding, X. Fu, Z. Li, *Angew. Chem. Int. Ed.* **2012**, *51*, 3364-3367; cP. Wu, C. He, J. Wang, X. Peng, X. Li, Y. An, C. Duan, *J. Am. Chem. Soc.* **2012**, *134*, 14991-14999; dM. Dan-Hardi, C. Serre, T. Frot, L. Rozes, G. Maurin, C. Sanchez, G. Ferey, *J. Am. Chem. Soc.* **2009**, *131*, 10857-10858.
- [6] H. Deng, C. J. Doonan, H. Furukawa, R. B. Ferreira, J. Towne, C. B. Knobler, B. Wang, O. M. Yaghi, *Science* **2010**, *327*, 846-850.
- [7] P. Horcajada, T. Chalati, C. Serre, B. Gillet, C. Sebrie, T. Baati, J. F. Eubank, D. Heurtaux, P. Clayette, C. Kreuz, J.-S. Chang, Y. K. Hwang, V. Marsaud, P.-N. Bories, L. Cynober, S. Gil, G. Ferey, P. Couvreur, R. Gref, *Nat. Mater.* **2010**, *9*, 172-178.
- [8] L. E. Kreno, K. Leong, O. K. Farha, M. Allendorf, R. P. Van Duyne, J. T. Hupp, *Chem. Rev.* **2012**, *112*, 1105-1125.
- [9] aW. Xuan, C. Zhu, Y. Liu, Y. Cui, *Chem. Soc. Rev.* **2012**, *41*, 1677-1695; bJ. Della Rocca, D. Liu, W. Lin, *Acc. Chem. Res.* **2011**, *44*, 957-968.
- [10] aS. Furukawa, K. Hirai, K. Nakagawa, Y. Takashima, R. Matsuda, T. Tsuruoka, M. Kondo, R. Haruki, D. Tanaka, H. Sakamoto, S. Shimomura, O. Sakata, S. Kitagawa, *Angew. Chem.* **2009**, *48*, 1766-1770; bX. Song, T. K. Kim, H. Kim, D. Kim, S. Jeong, H. R. Moon, M. S. Lah, *Chem. Mater.* **2012**, *24*, 3065-3073; cK. Koh, A. G. Wong-Foy, A. J. Matzger, *Chem. Commun.* **2009**, 6162-6164.
- [11] aS. Marx, W. Kleist, J. Huang, M. Maciejewski, A. Baiker, *Dalton Trans.* **2010**, *39*, 3795-3798; bA. A. Talin, A. Centrone, A. C. Ford, M. E. Foster, V. Stavila, P. Haney, R. A. Kinney, V. Szalai, F. El Gabaly, H. P. Yoon, F. Leonard, M. D. Allendorf, *Science* **2014**, *343*, 66-69.
- [12] U. Díaz, M. Boronat, A. Corma, *Proc. R. Soc. A.* **2012**, *468*, 1927-1954.
- [13] aA. Dazzi, R. Prazeres, F. Glotin, J. M. Ortega, M. Al-Sawaftah, M. de Frutos, *Ultramicroscopy* **2008**, *108*, 635-641; bB. Lahiri, G. Holland, A. Centrone, *Small* **2013**, *9*, 439-445; cB. Lahiri, G. Holland, V. Aksyuk, A. Centrone, *Nano Lett.* **2013**, *13*, 3218-3224; dA. M. Katzenmeyer, V. Aksyuk, A. Centrone, *Anal. Chem.* **2013**, *85*, 1972-1979; eJ. R. Felts, K. Kjolller, M. Lo, C. B. Prater, W. P. King, *ACS Nano* **2012**, *6*, 8015-8021; fA. Dazzi, F. Glotin, R. Carminati, *J. Appl. Phys.* **2010**, *107*, -; gA. Dazzi, R. Prazeres, F. Glotin, J. M. Ortega, *Infrared Phys. Technol.* **2006**, *49*, 113-121.
- [14] C. Volkringer, M. Meddouri, T. Loiseau, N. Guillou, J. Marrot, G. Ferey, M. Haouas, F. Taulelle, N. Audebrand, M. Latroche, *Inorg. Chem.* **2008**, *47*, 11892-11901.
- [15] S. Furukawa, K. Hirai, Y. Takashima, K. Nakagawa, M. Kondo, T. Tsuruoka, O. Sakata, S. Kitagawa, *Chem. Commun.* **2009**, 5097-5099.
- [16] T. Fukushima, S. Horike, H. Kobayashi, M. Tsujimoto, S. Isoda, M. L. Foo, Y. Kubota, M. Takata, S. Kitagawa, *J. Am. Chem. Soc.* **2012**, *134*, 13341-13347.
- [17] R. J. T. Houk, B. W. Jacobs, F. E. Gabaly, N. N. Chang, A. A. Talin, D. D. Graham, S. D. House, I. M. Robertson, M. D. Allendorf, *Nano Lett.* **2009**, *9*, 3413-3418.
- [18] X. Kong, H. Deng, F. Yan, J. Kim, J. A. Swisher, B. Smit, O. M. Yaghi, J. A. Reimer, *Science* **2013**, *341*, 882-885.

- [19] C. Marcott, M. Lo, K. Kjoller, C. Prater, I. Noda, *Appl. Spectrosc.* **2011**, *65*, 1145-1150.
- [20] B. Van Eerdenbrugh, M. Lo, K. Kjoller, C. Marcott, L. S. Taylor, *Mol. Pharm.* **2012**, *9*, 1459-1469.
- [21] C. Policar, J. B. Waern, M.-A. Plamont, S. Clède, C. Mayet, R. Prazeres, J.-M. Ortega, A. Vessières, A. Dazzi, *Angew. Chem. Int. Ed.* **2011**, *50*, 860-864.
- [22] D. Dubbeldam, K. S. Walton, D. E. Ellis, R. Q. Snurr, *Angew. Chem. Int. Ed.* **2007**, *46*, 4496-4499.
- [23] aA. F. Gross, E. Sherman, S. L. Mahoney, J. J. Vajo, *J. Phys. Chem. A* **2013**, *117*, 3771-3776; bM. Kim, J. F. Cahill, H. Fei, K. A. Prather, S. M. Cohen, *J. Am. Chem. Soc.* **2012**, *134*, 18082-18088; cM. Kim, J. F. Cahill, Y. Su, K. A. Prather, S. M. Cohen, *Chem. Sci.* **2012**, *3*, 126-130; dT. Li, M. T. Kozlowski, E. A. Doud, M. N. Blakely, N. L. Rosi, *J. Am. Chem. Soc.* **2013**, *135*, 11688-11691.
- [24] aL. Wu, M. Xue, S.-L. Qiu, G. Chaplais, A. Simon-Masseron, J. Patarin, *Microporous Mesoporous Mater.* **2012**, *157*, 75-81; bM. Savonnet, D. Bazer-Bachi, N. Bats, J. Perez-Pellitero, E. Jeanneau, V. Lecocq, C. Pinel, D. Farrusseng, *J. Am. Chem. Soc.* **2010**, *132*, 4518-4519.
- [25] R. N. Jones, C. Sandorfy, in *Technique of Organic Chemistry, Vol. IX* (Ed.: A. Weissberger), Interscience, New York, **1956**.
- [26] M. Savonnet, D. Farrusseng, **2011**.
- [27] C. Mayet, A. Dazzi, R. Prazeres, E. Allot, E. Glotin, J. M. Ortega, *Opt. Lett.* **2008**, *33*, 1611-1613.
- [28] B. L. Huang, Z. Ni, A. Millward, A. J. H. McGaughey, C. Uher, M. Kaviani, O. Yaghi, *Int. J. Heat Mass Transfer* **2007**, *50*, 405-411.